DNA on Chiral Surfaces

DOI: 10.1002/anie.200806295

Selective Adsorption of DNA on Chiral Surfaces: Supercoiled or Relaxed Conformation**

Hui Gan, Kangjian Tang, Taolei Sun, Michael Hirtz, Yong Li, Lifeng Chi,* Stefan Butz, and Harald Fuchs*

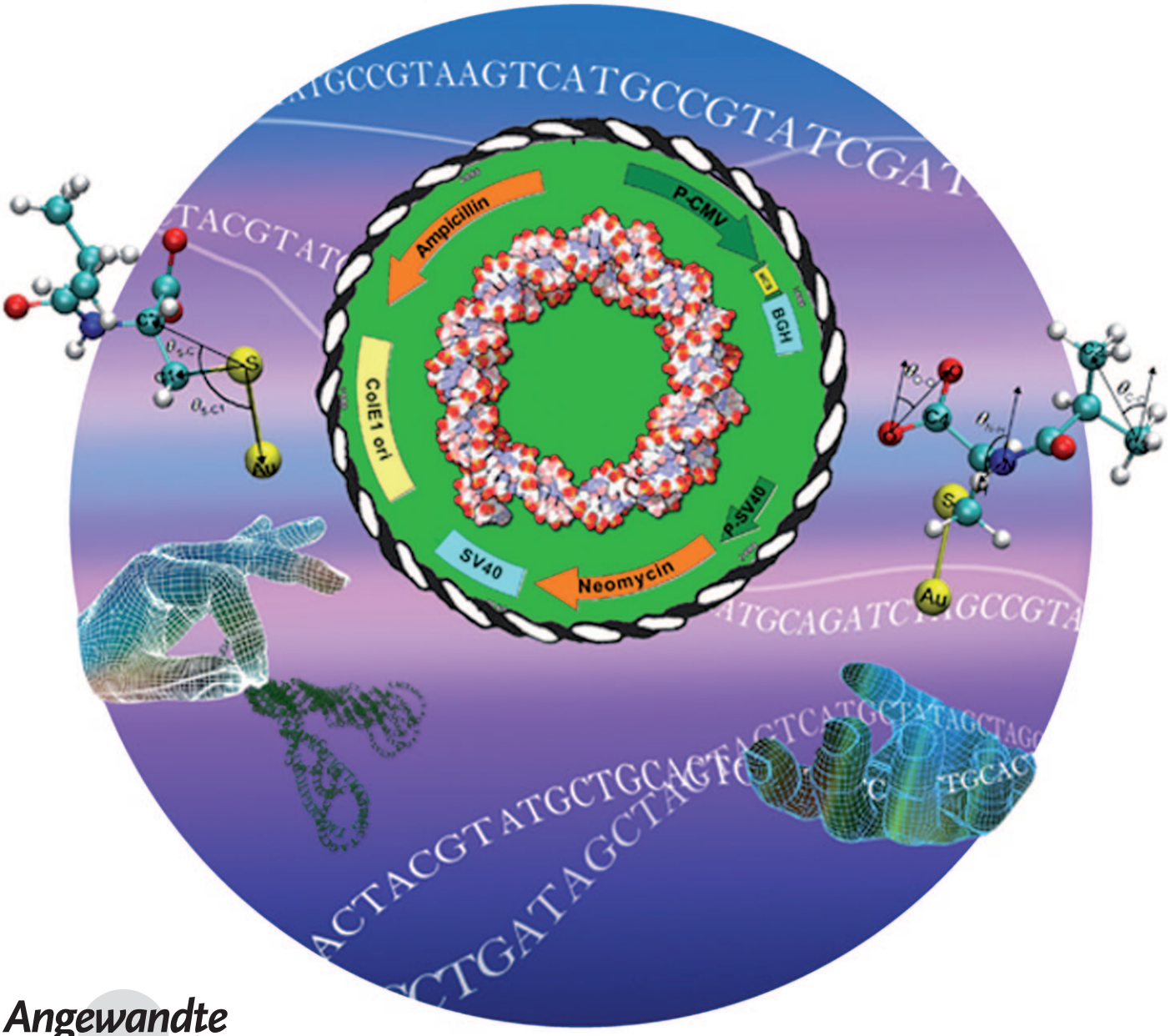

The DNA helix shows various conformations, which have significant influence on its biological functions and activities.[1–3] The selective recognition and manipulation of these conformations is important in many applications.[4–8] Chirality is one of the distinctive biochemical signatures of life.[9–11] It plays a decisive role in DNA behavior and in the interactions of DNA with guest molecules.[12–15] Herein we report on the selective adsorption of DNA on chiral surfaces. With a plasmid DNA molecule (pcDNA3) as a model, we demonstrate that, for gold surfaces modified with *N*-isobutyryl-L(D)-cysteine (NIBC) enantiomers, the L surface induces a transformation from the supercoiled conformation to relaxed conformations and has a strong interaction with adsorbed DNA molecules, while the interaction with the D surface is rather weak, and DNA strands maintain their supercoiled conformation on it. Theoretical simulation indicates that there are chirality-induced differences in molecular configurations for surface-bound L- and D-NIBC, and that these differences may be the origin of this effect. This finding will help us to better understand the interaction between DNA and other biochemical species, and it opens up a novel avenue for DNA-based devices[16] and relevant studies.[17,18]

A plasmid is a circular extrachromosomal DNA strand that is capable of replicating independently of the chromosomal DNA and is used as an important tool in genetics and biotechnology. It normally exists in four conformations: nicked open-circular, relaxed circular, linear, and supercoiled.[19] Owing to further twist and folding of the DNA double helix, the supercoiled conformation is quite compact, while for the other three conformations, DNA chains are loosely packed and thus are much more relaxed. Figure 1a shows a schematic diagram of the structure of pcDNA3. Figure 1b depicts the results of agarose gel electrophoresis of the DNA specimen obtained by the standard protocol provided by QIAGEN, in which a narrow band with a length around 5.4 kbp (kbp = 1000 base pairs) can be observed. This value is in good agreement with the theoretical value[20] and shows that most pcDNA3 molecules exhibit a supercoiled conformation and that the purity is high.

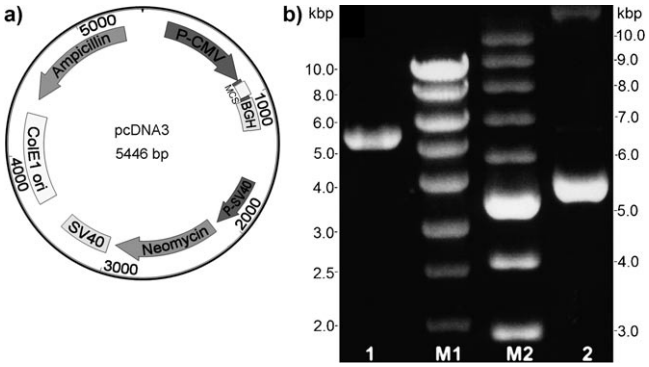

Figure 1. a) Schematic diagram for the structure of pcDNA3. b) Agarose gel analysis of the DNA specimen. Lanes 1 is a pcDNA3 specimen linearized by BamH digestion, which is used to determine the molecular weight of the sample, and lane 2 is the original circular pcDNA3 specimen. Lanes M1 and M2 are standard molecular weight marker (Smart ladder, Eurogentec) and supercoiled plasmid DNA ladder (Bayou, Biolabs), respectively. The results show that the pcDNA3 specimen used in this study has a molecular weight around 5.4 kbp and is composed mostly of the supercoiled conformation in solution.

As a derivative of cysteine, NIBC is an important biomolecule that has been used extensively in the chromatographic separation of chiral amino acids,[21] and it is one of the few chiral compounds that is commercially available in high purity and contains SH group. Herein, the enantiomers were used to modify the ultraflat gold substrates[22] through self-assembly by simply immersing the samples in ethanol solutions of D- or L-NIBC overnight to obtain chiral surfaces. Atom force microscopy (AFM) was utilized to study the morphology of the adsorbed plasmids after 4 h of incubation in an aqueous tris–EDTA solution of pcDNA3 with a concentration of about 10 $\mu g\,mL^{-1}$ at 25 °C (tris = tris(hydroxymethyl)aminomethane, EDTA = ethylenediaminetetraacetic acid). Figure 2a,b show typical AFM images for the adsorbed DNA molecules on L and D surfaces, respectively. Interestingly, although the chemical compositions of the two surfaces are the same, great differences in both the morphology and density for the adsorbed DNA molecules were observed. On the L surface, the DNA chains are quite relaxed and the adsorption density is rather high. Different relaxed conformations (mainly the relaxed circular conformation, upper inset of Figure 2a) can be observed in large quantity. The length of the DNA chains can be estimated by analyzing the AFM image. Most of the chains are in the range of approximately 1.4–1.6 μm, and the height is about 1–2 nm, as shown by the section profile of the AFM image (Figure 2a, lower inset). These data are in good agreement with the theoretical values for perimeter and thickness of pcDNA3, according to the total number of base pairs. Some supercoiled states can be occasionally observed, but their quantity is very low.

[*] Dr. H. Gan, Dr. K. Tang, Dr. T. Sun, M. Hirtz, Y. Li, Prof. Dr. L. Chi, Prof. Dr. H. Fuchs
Physikalisches Institut, WWU Münster
Wilhelm-Klemm-Strasse 10, 48149 Müster (Germany)
Fax: (+49) 251-83-33602
E-mail: sunt@uni-muenster.de
chi@uni-muenster.de
Dr. T. Sun, Prof. Dr. L. Chi, Prof. Dr. H. Fuchs
Center for Nanotechnology
48151 Münster (Germany)
Dr. S. Butz
Max-Planck-Institut für Molekulare Biomedizin
48149 Müster (Germany)
Dr. T. Sun
College of Chemistry and Molecular Sciences, Wuhan University
Wuhan 430072 (China)
Dr. H. Gan
Beijing Institute of Transfusion Medicine
Beijing 100850 (China)
[**] We thank for the Alexander von Humboldt (AvH) Foundation and the Federal Ministry of Education and Research of Germany (BMBF) for support (Sofja Kovalevskaja Award project).
Supporting information for this article is available on the WWW under http://dx.doi.org/10.1002/anie.200806295.

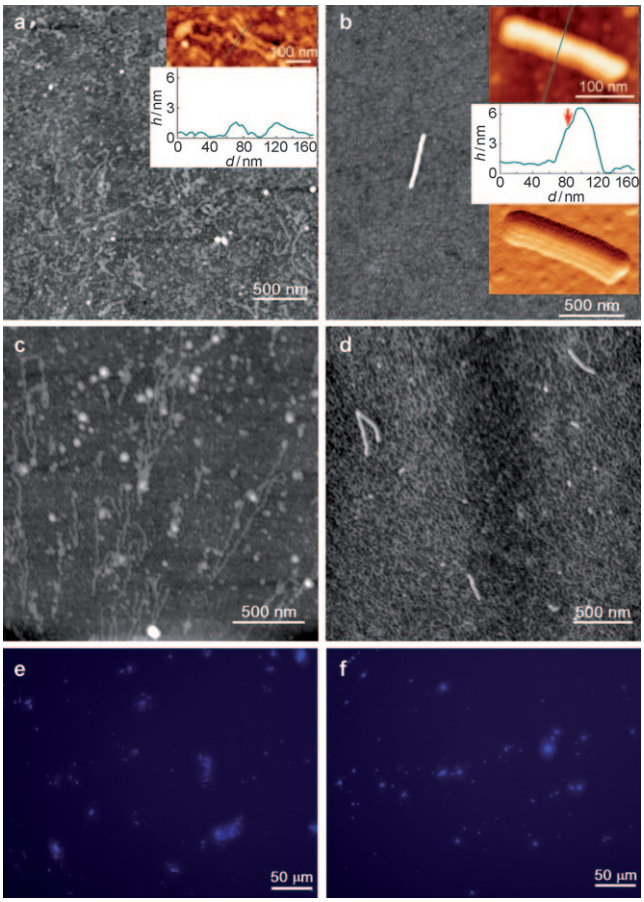

Figure 2. Different behavior of pcDNA3 on gold surfaces modified with L- (a, c, e) and D-NIBC (b, d, f). a), b) Comparison of the DNA morphology on the surfaces by AFM. Most DNA molecules exhibit relaxed conformations on the L surface, while on the D surface they adopt a supercoiled rod-like conformation. Insets in (a) are the magnified image of a single relaxed circular DNA molecule on the L surface and the corresponding section profile along the green line. The total length of the DNA molecule is about 1.4 μm and the height is about 1–2 nm. Insets in (b) are the magnified image of a supercoiled DNA rod on the D surface, and the corresponding section profile along the green line and amplitude image. The length of the rod is about 200 nm and its height is about 6.6 nm. Its step-like structure (red arrow) can be clearly observed. c), d) Similar AFM results obtained in the presence of Mg^{2+} ions (10 μmol ml^{-1}). e), f) Fluorescence microscopy results showing a macroscopic difference for the adsorption behavior of DNA on chiral surfaces.

The situation on the D surface is totally different. The relaxed conformations are very rare. Instead, there are a considerable number of short but thick rod-like plasmids on the surface (Figure 2b). The structure is uniform and regular. Most rods show a fixed length of approximately 400 or 260 nm. Shorter (ca. 200 nm) or longer rods (600–800 nm) can also be observed, but there are fewer of them. Interestingly, the lengths of these rods match those predicted for multi-folded states (for example, 400 and 260 nm correspond well to the 4- and 6-folded states, respectively) of the circular plasmid based on the theoretical length of the fully relaxed state. The upper inset of Figure 2b shows the magnified image of a single DNA rod with a length of about 200 nm using a Q-control mode of AFM with reduced interaction between the tip and the sample.[23] The corresponding section profile (middle inset of Figure 2b) reveals that the height of most DNA rods is in the range of 4–7 nm, which is significantly higher than the relaxed states on the L surface. For different DNA rods, the height increases roughly with the decrease in length. Multilayer structures can be clearly observed, as revealed by the steps (arrow) in the section profile and the corresponding amplitude image (lower inset of Figure 2b), which illustrates the folding of the DNA chain in the vertical direction.

The above results indicate that the surface chirality has a dramatic influence on the behavior of DNA on a surface. Since Mg^{2+} ions are reported to have great influence on DNA behavior and on the interaction with other molecules,[24] we did the same experiments in the presence of Mg^{2+} ions at a concentration of about 10 μmol ml^{-1} in solution. As shown in Figure 2c,d, similar phenomena as before were observed, while the surface density of the adsorbed DNA is higher than without Mg^{2+} ions for both surfaces. These results indicate that the effect of chirality is so predominant that even the addition of a certain concentration of Mg^{2+} ions cannot cover up the effect.

We further used fluorescence microscopy to investigate the macroscopic profile of the chirality effect. The DNA molecules were labeled by a fluorescent dye (Hoechst 33342) before observation by microscopy. In this experiment, although it is impossible to distinguish individual DNA molecules owing to the resolution limitations, great differences can still be observed for the two surfaces. As shown in Figure 2e, the DNA molecules on the L surface show a cloud-like image with ambiguous edges. In contrast, those on the D surface (Figure 2f) are quite separate and show particle-like images, the edges of which are rather sharp. These profiles are in good accordance with the relaxed and supercoiled conformations of DNA in the AFM experiments, thus further confirming the effect from a macroscopic point of view. Considering that the pcDNA3 molecules mainly exist in the supercoiled conformation in solution in our experiment, it can be inferred that there is a relatively strong interaction between DNA molecules and the L surface, which results in a high adsorption density on the surface and induces the transformation of DNA molecules from the supercoiled conformation to the relaxed conformations. However, on the D surface, the interaction is so weak that DNA molecules prefer to preserve the supercoiled conformation when adsorbed onto the surface.

The amount of adsorbed DNA is another important parameter to evaluate the interaction between the adsorbed molecules and the surface. Figure 3 shows a comparison for the amount of adsorbed DNA on D and L surfaces for different DNA concentrations. The evaluation was carried out using a UV/Vis spectrophotometric method[25] by analyzing the intensity of the absorption peak at 260 nm. A distinctly higher amount of adsorption (T test, $p < 0.01$ for all concentrations) on the L surface than the D surface is detected, and the difference increases with increasing DNA concentration. These data support the difference in adsorption density found in AFM experiments. All of the above data are consistent and

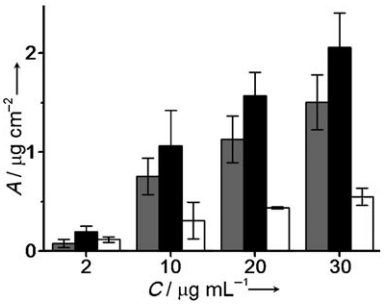

Figure 3. Adsorption *A* of pcDNA3 on the chiral surfaces versus DNA concentration *C* as determined by UV/Vis spectroscopy. Gray: D surface; black: L surface; white: difference between D and L surfaces. Significantly more DNA adsorbs on the L surface than on the D surface (*T* test, $p < 0.01$), and the difference increases with increasing DNA concentration.

clearly demonstrate the stereospecific interaction between the plasmid and chiral surfaces. Similar phenomena were also observed for a single-stranded DNA specimen,[26] thus indicating that this effect is not unique to specific DNA molecules but may be a general effect.

Chirality is intrinsically present in DNA structure at both the molecular and supermolecular levels, and it plays a decisive role in the interaction with other biochemical species.[12–14] The effect described herein thus provides an interesting insight to understand such interactions. Hydrogen bonding and hydrophobic interactions are important for the physical and chemical behavior of DNA molecules as well as for the intercalation of guest molecules in double-stranded DNA.[27–29] Owing to the existence of COOH and NH groups that are connected to chiral carbon atoms and to the presence of the large hydrophobic isobutyryl group connected to the NH group in NIBC, we assume that the above phenomena may be caused by the configurational matching or mismatching between the chiral moieties in DNA and the NIBC enantiomers on the surface.

With this idea in mind, we further used molecular dynamics calculations to simulate the molecular configurations of NIBC molecules on a surface in an aqueous environment, in which the GROMACS program[30] combined with the AMBER field[31] was selected for the simulation. Interestingly, although the mirror-image configurations (Figure 4a,b) were used as the starting point, significant differences in the configurations can be observed for L- and D-NIBC on the gold surface, resulting in arrangements that are no longer mirror images. Statistically, NIBC molecules show two main kinds of configurations on both surfaces, while the proportion for the major one (as characterized by a small average rotation angle ϕ of the COOH group around the chiral carbon atom, Figure 4c), which is more flexible for rotation of the isobutyryl group, is significantly higher on the L surface than on the D surface. Furthermore, for each configuration, the exact values for ϕ and the inclination of molecules (angle θ_{S-C}, Figure 4d) and orientations for NH, COOH, and isopropyl groups (average values for angles θ_{S-C}, θ_{N-H}, θ_{O-O} and θ_{C-C}, Figure 4d,e) are also different considering the chirality (see the Supporting Information for details). Although the detailed mechanism[32] is still unclear (it is one important

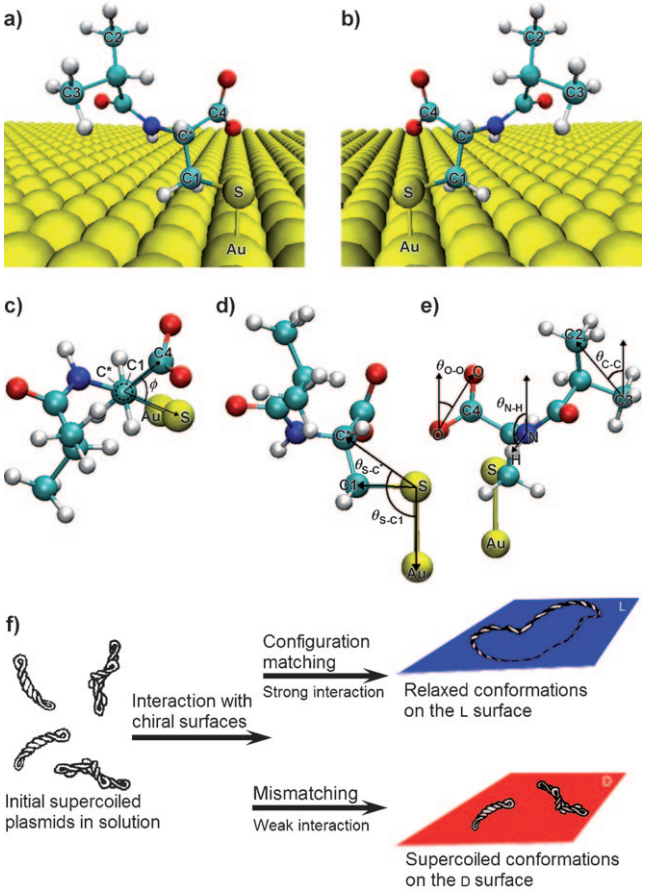

Figure 4. a)–e) Molecular dynamics simulation for configurations of NIBC molecules on surfaces. f) Schematic diagram of the possible mechanism for the stereospecific interaction between DNA and chiral surfaces. a), b) Starting configurations used before simulation for L- and D-NIBC, respectively; they are mirror images. c)–e) Parameters used in the simulation to assess the configurational difference between surface-bound L- and D-NIBC molecules. ϕ represents the rotation of groups surrounding the chiral carbon atom (C*), which is defined as the angle between the projections of vectors C*→C4 and C1→S. Angles θ_{S-C} are used to evaluate the overall inclination of NIBC molecules to the surface, in which θ_{S-C*} is defined as the angle between vectors S→Au and S→C* and θ_{S-C1} is that between vectors S→Au and S→C1. Angles θ_{N-H}, θ_{O-O}, θ_{C-C} are used to characterize orientations of the NH, COOH, and isopropyl groups and are defined as angles between the vertical direction and vectors N→H, O→O, C3→C2, respectively. Significant differences in these parameters were found for L- and D-NIBC after simulation, even though the chirality difference had already been considered, revealing different configurations for the surface-bound enantiomers. See the Supporting Information for details. The different interactions between DNA molecules and L and D surfaces are considered to be induced by matching or mismatching between the molecular configurations of the NIBC enantiomers and DNA.

focus of our future work), we hypothesize that the differences in molecular configurations, as well as the specific chiral arrangement of the groups, may greatly influence the binding and interaction between DNA and L- and D-NIBC molecules on gold surfaces (Figure 4f). The molecular configuration of L-NIBC may match well with the DNA molecule and can bind with the major or minor grooves of DNA through hydrogen

bonding and hydrophobic interactions, leading to a strong interaction between DNA molecules and the surface; however, for D-NIBC, the binding is not easy because the configurations do not match, thus resulting in a weak interaction between DNA and the surface.

The above results reveal a potential chirality-based strategy to control and separate different conformations of DNA on a surface, which is important for DNA manipulation and DNA-based devices, thus opening up a novel avenue for relevant studies. On the other hand, owing to the ubiquity of chirality in living systems and its important role in biochemical processes, detailed mechanistic analysis of the above effect can help us to better understand the interaction between DNA and other biochemical species. Furthermore, in the context of stereospecific interaction between biological cells and chiral surfaces,[11] the selective behavior of DNA or other biomacromolecules on chiral surfaces can provide useful information to comprehend such phenomena and the high chiral preference in living systems.

In conclusion, we report the stereoselective adsorption of plasmids on chiral surfaces modified with NIBC enantiomers. Plasmids exhibit relaxed conformations on the L surface, and the extent of adsorption is higher; on the D surface, they prefer to stay in a supercoiled conformation with a very compact rod-like morphology, and the extent of adsorption is lower. Simulation results show that the chirality-induced difference in the molecular configurations for surface-bound L- and D-NIBC molecules is the origin of this effect, which greatly influences their interactions with DNA molecules. This study opens up a novel avenue for the design of DNA-based devices or other relevant studies, and it helps to further our understanding of the interaction between DNA and other biochemical species and of the corresponding bioprocesses at the cell level.

Experimental Section

Experimental details can be found in the Supporting Information. In brief, the plasmid pcDNA3 specimen was transformed and propagated in *Escherichia coli* DH5α by standard protocol. Large-scale pure plasmids were obtained from QIAfilter Maxi Plasmid Purification Kits (QIAGEN Ltd, Germany). Agarose gel electrophoresis was performed on Biotec Fischer products (UK). In AFM experiments, ultraflat sputtered gold substrates were used, which were modified with L- and D-NIBC by self-assembly to give chiral surfaces. The experiments were performed on a NanoScope IIIa Scanning Probe Microscope (Digital Instruments) in tapping mode at room temperature. The amount of adsorbed DNA on the chiral surfaces was evaluated quantitatively by UV/Vis spectroscopy. The fluorescence microscopy images were obtained after the samples were labeled by Hoechst 33342 dye. The molecular dynamics simulation for the molecular configurations of surface-bound L- and D-NIBC was performed by the GROMACS program combined with the AMBER field.

Received: December 23, 2008
Revised: February 11, 2009
Published online: March 23, 2009

Keywords: chirality · conformation analysis · DNA · stereoselective interaction · surface chirality

[1] M. T. Record, S. J. Mazur, P. Melancon, J. H. Roe, S. L. Shaner, L. Unger, *Annu. Rev. Biochem.* **1981**, *50*, 997 – 1024.
[2] "Structure of DNA and RNA": M. Siram, A. J. Wang in *Bioorganic Chemistry—Nucleic Acids* (Ed.: S. M. Hecht), Oxford University Press, Oxford, **1996**.
[3] J. J. Champoux, *Annu. Rev. Biochem.* **2001**, *70*, 369 – 413.
[4] G. R. Smith, *Cell* **1981**, *24*, 599 – 600.
[5] F. Kouzine, D. Levens, *Front. Biosci.* **2007**, *12*, 4409 – 4423.
[6] K. Remaut, N. N. Sanders, F. Fayazpour, J. Demeester, S. C. De Smedt, *J. Controlled Release* **2006**, *115*, 335 – 343.
[7] D. Remus, E. L. Beall, M. R. Botchan, *EMBO. J.* **2004**, *23*, 897 – 907.
[8] C. M. Niemeyer, M. Adler, *Angew. Chem.* **2002**, *114*, 3933 – 3937; *Angew. Chem. Int. Ed.* **2002**, *41*, 3779 – 3783.
[9] R. M. Hazen, D. S. Scholl, *Nat. Mater.* **2003**, *2*, 367 – 374.
[10] M. Levin, M. Mercola, *Genes Dev.* **1998**, *12*, 763 – 769.
[11] T. Sun, D. Han, K. Riehemann, L. Chi, H. Fuchs, *J. Am. Chem. Soc.* **2007**, *129*, 1496 – 1497.
[12] S. Sforza, G. Galaverna, A. Dossena, R. Corradini, R. Marchelli, *Chirality* **2002**, *14*, 591 – 598.
[13] X. Qu, J. O. Trent, I. Fokt, W. Priebe, J. B. Chaires, *Proc. Natl. Acad. Sci. USA* **2000**, *97*, 12032 – 12037.
[14] H. C. Becker, B. Nordén, *J. Am. Chem. Soc.* **2000**, *122*, 8344 – 8349.
[15] R. Corradini, S. Sforza, T. Tedeschi, R. Marchelli, *Chirality* **2007**, *19*, 269 – 294.
[16] C. Bustamante, Z. Bryant, S. B. Smith, *Nature* **2003**, *421*, 423 – 427.
[17] S. Wang, H. Liu, D. Liu, X. Ma, X. Fang, L. Jiang, *Angew. Chem.* **2007**, *119*, 3989 – 3991; *Angew. Chem. Int. Ed.* **2007**, *46*, 3915 – 3917.
[18] H. Liu, Y. Xu, F. Li, Y. Yang, W. Wang, Y. Song, D. Liu, *Angew. Chem.* **2007**, *119*, 2567 – 2569; *Angew. Chem. Int. Ed.* **2007**, *46*, 2515 – 2517.
[19] C. Ke, Y. Jiang, P. A. Mieczkowski, G. G. Muramoto, J. P. Chute, P. E. Marszalek, *Small* **2008**, *4*, 288 – 294.
[20] The sequence and structure of plasmid pcDNA3 were compiled from information in Invitrogen's Technical Services Department.
[21] H. Brückner, S. Haasmann, M. Langer, T. Westhauser, R. Wittner, *J. Chromatogr. A* **1994**, *666*, 259 – 273.
[22] M. Hegner, P. Wagner, G. Semenza, *Surf. Sci.* **1993**, *291*, 39 – 46.
[23] S. Gao, L. Chi, S. Lenhert, B. Anczykowski, C. M. Niemeyer, M. Adler, H. Fuchs, *ChemPhysChem* **2001**, *2*, 384 – 388.
[24] V. V. Rybenkov, A. V. Vologodskii, N. R. Cozzarelli, *J. Mol. Biol.* **1997**, *267*, 299 – 311.
[25] K. A. Haque, R. M. Pfeiffer, M. B. Beerman, J. P. Struewing, S. J. Chanock, A. W. Bergen, *BMC Biotechnol.* **2003**, *3*, 20.
[26] K. Tang, H. Gan, Y. Li, L. Chi, T. Sun, H. Fuchs, *J. Am. Chem. Soc.* **2008**, *130*, 11284 – 11285.
[27] Z. Morávek, S. Neidle, B. Schneider, *Nucleic Acids Res.* **2002**, *30*, 1182 – 1191.
[28] M. Y. Tolstorukov, R. L. Jernigan, V. B. Zhurkin, *J. Mol. Biol.* **2004**, *337*, 65 – 76.
[29] B. Nguyen, S. Neidle, W. D. Wilson, *Acc. Chem. Res.* **2009**, DOI: 10.1021/ar800016q.
[30] D. Van der Spoel, E. Lindahi, B. Hess, G. Groenhof, A. E. Mark, H. J. C. Berendsen, *J. Comput. Chem.* **2005**, *26*, 1701 – 1718.
[31] J. Wang, P. Cieplak, P. A. Kollman, *J. Comput. Chem.* **2000**, *21*, 1049 – 1074.
[32] P. Szabelski, *Chem. Eur. J.* **2008**, *14*, 8312 – 8321.

